Physics-Based Analytical Modeling of Electromigration Reliability for Multi-Segment Interconnect Wires

***Abstract*—Electromigration (EM) is the major concern for the VLSI back end of the line (BEOL) reliability. For EM modeling and assessment, one important problem is to perform fast EM time to failure analysis for practical interconnect layouts such as clock and power/ground networks consisting of many multi-segment wires. However, existing EM modeling and analysis techniques are mainly developed for a single wire. Although there are some early effects to resolve this issue, but there is no general analytic and compact model developed to estimate the EM-induced stress evolution, which is required to predict the time to failure. In this paper, we propose a new analytic expression hydrostatic stress calculation for general multi-segment interconnect wire with multiple terminals. The new method is based on the Laplace transformation method on the Korhonen's equation with blocked atom flux boundary conditions. The analytical solutions in terms of a set of auxiliary basis functions using the complementary error function agree well with the numerical analysis results. Our analysis further demonstrates that using the first one dominant basis function approximation can lead to 2% error, which is sufficient for practical EM analysis.**

I. Introduction

Electromigration is considered as the top killer for today's copper dual damascene interconnect technology. Recently there is a renewed interest in EM modeling and mitigation techniques as EM-induced reliability is getting worse as technology advance. ITRS predicts that the EM-induced lifetime of the interconnects will be reduced by half by each generation [1]. To make this situation worse, many widely used EM models such as Black-Blech models are thought to be too conservative, which can lead to significant over designs [2].

Existing EM model and analysis techniques mainly focus on the simple straight line interconnect with two line end terminals [3]. Existing widely used EM models such as Blech limit [4] (for the out filtration of immortal segments) and Black's equation [5] (for calculating MTTFs for segments characterized by known current densities and temperatures) are subjects of the hard criticism [6] [7] [8] as those empirical models are stressing condition dependent and lacks of scalability over wide current and temperature stressing conditions. More importantly, those models can only be applied to simple wire structures. For practical VLSI chips, the interconnects such as clock and power grid networks typically consist of multi-branch metal segments representing continuously connected, highly conductive metal (Cu) lines within one layer of metallization, terminating at diffusion barriers, which are commonly seen in the power/ground networks. The EM effects in those branches are not independent and they have to be considered simultaneously. To further illustrate this, we consider a 4-segment and 5-terminal interconnect wire loaded with DC voltage distribution as shown in Fig. 1. The finite element analysis (FEA) can be used to calculate EM-induced hydrostatic stress along the interconnect wire. The distributions of the hydrostatic stress (top), current density (middle) and voltage potential (bottom) along this wire are shown in Fig. 2 respectively. As we can see that although the segment 2 has almost zero current density, its tensile (positive) stress is the highest. Hence it is no longer valid to analyze the EM-induced back stress for each individual wire segment separately as with existing methods. As a result, we have to analyze all the stress evolution as a whole instead of treating each segment separately as done in the existing EM assessment methods.

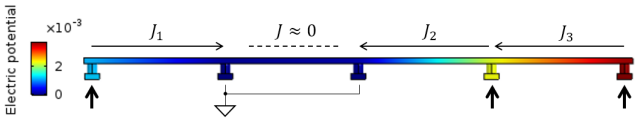

Fig. 1. Electrical current in a 4-segment wire structure (J: current direction).

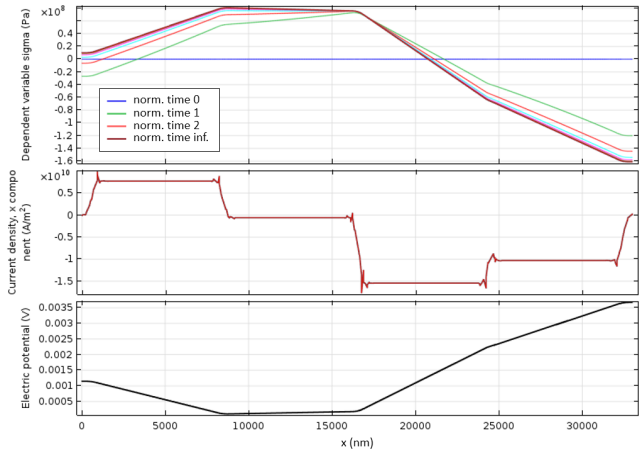

Fig. 2. Hydrostatic stress, current density, and voltage distribution in the 4-segment wire structure.

Recently some physics-based EM analysis methods for the TSV and power grid networks have been proposed based on solving the basic mass transport equations [9]–[12]. Those models treat the resistance changes of a wire over time as the atomic concentration changes due to atomic flux. Since these proposed methods solve the basic mass transport equations using the finite element method, they can only solve for very

small structures such as one TSV structure. A complicated look-up table or models have to be built for different TSVs and wire segments for full-chip power grid analysis at reduced accuracy.

To mitigate this problem, a more compact physics-based EM model was proposed recently in [13] based on the hydrostatic stress diffusion equation [14]. However, this EM model still works for one single wire segment. Although the new EM model has been extended to deal with multiple branch tree wire based on projected steady-state stress, it still cannot provide the time-dependent hydrostatic evolution of hydrostatic stress, which ultimately determines the failures for multi-branch interconnect wires. Recently EM models for multi-branch interconnect tree have been proposed [15], [16]. In this approach, analytic solutions for stress evolution were derived for a few specific interconnect structures. Moreover, those analytic expressions still cannot be applied to more general structures such as the multi-segment interconnect wires shown in Fig. 1.

In this paper, we aim to resolve the mentioned problems for EM model. We propose a new analytic expression hydrostatic stress calculation for general multi-segment interconnect wire with multiple terminals. The new method is based on the Laplace transformation method on the Korhonen's equation with blocked atom flux boundary conditions. The analytical solutions in terms of a set of auxiliary basis functions using the complementary error function agree well with the numerical analysis results. Our analysis further demonstrates that using the first dominant basis function can lead to 2% error, which is sufficient for practical EM analysis.

The remainder of the paper is organized as follows. In Section II, we induce the physics-based EM models and analysis methods for the stress evolution during EM in simple interconnect wires. Then we present the new analytic model for a general multi-segment interconnect wire in Section III. Experiment results and discussions for the multi-segment interconnect wire examples and accuracy comparison against COMSOL-based finite element analysis are presented in Section IV. Concluding remarks are drawn in Section V.

II. Review of physics-based EM modeling and analysis methods

EM is a physical phenomenon of the migration of metal atoms along a direction of the applied electrical field. This oriented atomic flow, which is caused mostly by the momentum exchange between atoms and the conducting electrons, results in metal density depletion at the cathode, and a corresponding metal accumulation at the anode end of the metal wire. Due to the passivation of copper wires from the dual damascene copper interconnect technology, hydrostatic stress will build up from the metal concentration changes at those nodes, which will lead to void nucleation when the stress reach to the critical stress and following up failures of the wires as results of the void growth.

EM phenomena and EM modeling have been intensively studied and some important physics-based EM models have been proposed in the past two decades [3]. Korhonen proposed the important EM model to describe the EM-induced stress evolution of passivated interconnect wires and its analytic solution for a simple wire structure in 1993 [14], which was further developed by many researchers [17], [18]. Specifically, for a confined/passivated metal line, the hydrostatic stress distribution $\sigma(x,t)$ along the metal wire can be described by a one-dimensional diffusion-like equation, given by: [14]

$$\frac{\partial \sigma(x,t)}{\partial t} = \frac{\partial}{\partial x}\left[\kappa\left(\frac{\partial \sigma(x,t)}{\partial x} + G\right)\right] \tag{1}$$

where $\kappa = \frac{D_a B \Omega}{kT}$ is the stress diffusivity affected by temperature T and $G = \frac{Z^* e \rho}{\Omega} j$ is the EM driving force. Moreover, $D_a = D_0 e^{-\frac{E_a}{kT}}$ is the effective atomic diffusion coefficient. D_0 and E_a stand for the pre-exponential factor and the activation energy, respectively. The Korhonen equation (1) has different analytical solutions with different boundary conditions (BCs). Following the idea in [14], we assume that the stress diffusivity κ does not depend on time. During the void nucleation phase of EM, the atom fluxes are blocked at both wire ends $x = 0$ and $x = L$ at any moment in time. The initial stress value during the void nucleation phase is set to be zero. Thus, the closed-form solution of the stress evolution equation for a single segment wire can be given as follows [14]:

$$\begin{aligned}\sigma(x,t) = \sigma_T + GL\{&\frac{1}{2} - \frac{x}{L} \\ &- 4\sum_{n=0}^{\infty} \frac{\cos((2n+1)\pi\frac{x}{L})}{(2n+1)^2\pi^2 \exp((2n+1)^2\pi^2\frac{\kappa t}{L^2})}\}.\end{aligned} \tag{2}$$

where σ_T is the pre-existing residual stress due to a thermal process. If we only keep the slowest decaying term of the infinite series in (2), we can compute the time to nucleation. This happens when the wire stress $\sigma(x,t)$ has reached a critical stress σ_{crit}, then the void nucleation time t_{nuc} can be obtained by solving the equation $\sigma(x, t_{nuc}) = \sigma_{crit}$ [13].

The physics-based EM model proposed in [13], [19] was extended further to deal with multi-branch interconnects, in which the projected steady-state EM-induced stress of each branch without considering other branches is first computed. Then the branch stresses are used to compute the total stress distributions in a tree for calculating the final time to failure if some of the stress is larger than the critical stress. The drawback of this work is that it totally ignores all the dynamic evolutions of stress over time and the interactions of void nucleation process among branches. As a result, it still cannot provide analytic expression for the time-dependent hydrostatic evolution of hydrostatic stress to determine the failures for multi-branch interconnect wires.

Recently, a voltage-based EM modeling and immortality check technique for general interconnect tree structures has been proposed [20]. In this work, the steady-state hydrostatic stress continuous equations are formed first and the steady state stress at every node of the tree are then computed in terms of node voltages and wire layout parameters. By checking the largest stress over all the tree nodes, one can ensure that the tree never fails if the largest stress is less than the critical stress. It is very helpful for fast EM immortality check. But, this method still can't give the time when the wire is

predicted to fail. Following a different direction, a research effort was carried out recently to develop time-dependent stress evolution analytic solution for multi-branch interconnect tree [15], [16]. In this approach, analytic solutions by means of the Laplace transformation method for stress evolution were derived for three specific interconnect structures: the straight-line 3-terminal wires, the T-shape 4-terminal wires and the cross-shape 5-terminal wires. It was also shown that a few dominant terms can be used for sufficiently accurate solution. But, the proposed solution is not still general enough for multi-segment interconnect wires shown in Fig. 1.

III. Accurate Analytical Modeling for Hydrostatic Stress Evolution

In this section, we present the new analytic solution and compact models for EM-induced stress evolution in confined multi-segment interconnect wires as shown in Fig. 1. To facilitate our analysis, we are looking at an abstract general multi-segment interconnect structure with one continuous metallization layer shown in Fig.3, which represents a long metal wire with n segments and $n+1$ terminals (vias) (presented by blue blocks) connecting different metal layers. Since many complex interconnect structures such as power grids could be decomposed hierarchically into smaller interconnect tree components like this structure, the accurate analytic closed-form expressions describing hydrostatic stress evolution for multi-branch interconnect trees will lay the groundwork for the EM reliability analysis of those global interconnect networks.

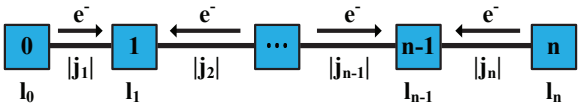

Fig. 3. An example of general realistic interconnect structure.

A. The analytic solution for stress evolution for multi-segment interconnect wires

The stress evolution process for each segment in Fig.3 can be described by a single Korhonen's equation as shown in (1). But solving such equation directly is more difficult. Instead, in our approach, we decouple the original single Korhonen's equation into n decoupled Korhonen equations and each of them governing one segment of the multi-segment wire. The partial differential equations (PDE) are linked by the boundary conditions representing the continuity of stress and fluxes at the junctions in the long metal wire. Specifically, the PDE in (1) can re-written into a number of decoupled PDEs as follows:

$$\begin{aligned}
&\frac{\partial \sigma_1}{\partial t} = \frac{\partial}{\partial x}[\kappa_1(\frac{\partial \sigma_1}{\partial x} + G_1)],\ l_0 \le x \le l_1\\
&\frac{\partial \sigma_2}{\partial t} = \frac{\partial}{\partial x}[\kappa_2(\frac{\partial \sigma_2}{\partial x} + G_2)],\ l_1 \le x \le l_2,\\
&\cdots\cdots\\
&\frac{\partial \sigma_{n-1}}{\partial t} = \frac{\partial}{\partial x}[\kappa_{n-1}(\frac{\partial \sigma_{n-1}}{\partial x} + G_{n-1})],\ l_{n-2} \le x \le l_{n-1},\\
&\frac{\partial \sigma_n}{\partial t} = \frac{\partial}{\partial x}[\kappa_n(\frac{\partial \sigma_n}{\partial x} + G_n)],\ l_{n-1} \le x \le l_n.
\end{aligned} \tag{3}$$

In (3), κ_i and G_i $(i = 1, 2, \cdots, n)$ are the stress diffusivity and the EM driving force for each segment wire. Boundary conditions for these equations are given as follows:

$$\begin{aligned}
&\kappa_1(\frac{\partial \sigma_1}{\partial x} + G_1) = 0,\ x = l_0,\\
&\sigma_1 = \sigma_2,\ x = l_1,\\
&\kappa_1(\frac{\partial \sigma_1}{\partial x} + G_1) = \kappa_2(\frac{\partial \sigma_2}{\partial x} + G_2),\ x = l_1,\\
&\sigma_2 = \sigma_3,\ x = l_2,\\
&\kappa_2(\frac{\partial \sigma_2}{\partial x} + G_2) = \kappa_3(\frac{\partial \sigma_3}{\partial x} + G_3),\ x = l_2,\\
&\cdots\cdots\\
&\kappa_n(\frac{\partial \sigma_n}{\partial x} + G_n) = 0,\ x = l_n.
\end{aligned} \tag{4}$$

Initial conditions for the void nucleation phase are given by $\sigma_i = 0$ at $t = 0$ at each segment.

To solve the resulting decoupled equations in (3) subject to the boundary conditions (4), the Laplace transformation technique is used to convert the PDE into the Laplace domain. For the sake of simplicity, we assume that $\kappa_1 = \kappa_2 = \cdots = \kappa_n$ and the EM driving force G_i does not depend on the time t and the position x. After transforming (3)-(4) by the Laplace transformation technique, we get a system of ordinary differential equations (ODEs):

$$\begin{aligned}
&\frac{d^2\hat{\sigma}_1(x,s)}{dx^2} = \frac{s}{\kappa_1}\hat{\sigma}_1(x,s),\ l_0 \le x \le l_1,\\
&\frac{d^2\hat{\sigma}_2(x,s)}{dx^2} = \frac{s}{\kappa_2}\hat{\sigma}_2(x,s),\ l_1 \le x \le l_2,\\
&\cdots\cdots\\
&\frac{d^2\hat{\sigma}_{n-1}(x,s)}{dx^2} = \frac{s}{\kappa_{n-1}}\hat{\sigma}_{n-1}(x,s),\ l_{n-2} \le x \le l_{n-1},\\
&\frac{d^2\hat{\sigma}_n(x,s)}{dx^2} = \frac{s}{\kappa_n}\hat{\sigma}_n(x,s),\ l_{n-1} \le x \le l_n,
\end{aligned} \tag{5}$$

where $\hat{\sigma}_i(x,s) = \int_0^{+\infty} e^{-st}\sigma_i(x,t)dt$ $(i = 1, 2, \cdots, n)$ is the Laplace transform of $\sigma_i(x,t)$. By using the Laplace transform of the boundary conditions (4), the analytical solution $\hat{\sigma}_i(x,s)$ of (5) can be obtained in the Laplace domain. Due to limit space, we omit the derivation process of obtaining $\hat{\sigma}_i(x,s)$.

By taking the inverse Laplace transform of $\hat{\sigma}_i(x,s)$, we can obtain the analytical solution $\sigma_i(x,t)$ for each PDE in (3). Before we present the concrete expression of $\sigma_i(x,t)$, we introduce the following notations:

$$\begin{aligned}
&\xi^i_{n,1}(m,x) = l_n + 2m(l_n - l_0) - x,\\
&\xi^i_{n,2}(m,x) = (2l_n - l_0) + 2m(l_n - l_0) - x,\\
&\xi^i_{n,2p+1}(m,x) = (2l_n - l_p) + 2m(l_n - l_0) - x,\\
&\xi^i_{n,2p+2}(m,x) = \begin{cases} (2l_n - 2l_0 + l_p) + 2m(l_n - l_0) - x, \\ \qquad\qquad\qquad 1 \le p < i, \\ l_p + 2m(l_n - l_0) - x,\ i \le p \le n-1, \end{cases}\\
&\eta^i_{n,1}(m,x) = (l_n - 2l_0) + 2m(l_n - l_0) + x,\\
&\eta^i_{n,2}(m,x) = -l_0 + 2m(l_n - l_0) + x,\\
&\eta^i_{n,2p+1}(m,x) = (l_p - 2l_0) + 2m(l_n - l_0) + x,\\
&\eta^i_{n,2p+2}(m,x) = \begin{cases} -l_p + 2m(l_n - l_0) + x,\ 1 \le p < i, \\ (2l_n - l_p - 2l_0) + 2m(l_n - l_0) + x, \\ \qquad\qquad\qquad i \le p \le n-1, \end{cases}
\end{aligned} \tag{6}$$

where m is a nonnegative integer, n is the number of segments, i $(i = 1, 2, \cdots, n)$ is the index of current segment, and p is an integer from 1 to $n-1$.

Similar to the analytical method introduced in [15], we first introduce the following basic function:

$$g(x,t) = 2\sqrt{\frac{\kappa t}{\pi}} e^{-\frac{x^2}{4\kappa t}} - x \times \mathtt{erfc}\{\frac{x}{2\sqrt{\kappa t}}\}. \tag{7}$$

where the complementary error function $\mathtt{erfc}\{x\}$ is defined as $\mathtt{erfc}\{x\} = \frac{2}{\sqrt{\pi}} \int_x^{+\infty} e^{-t^2} dt$.

With those definitions, it turns out that a general form of analytical solutions of stress evolution equations for the i-th $(i = 1, 2, \cdots, n)$ segment can be derived as follows

$$\begin{aligned}
\sigma_i(x,t) = &- \sum_{m=0}^{+\infty} \{G_n g(\xi^i_{n,1}(m,x),t) - G_1 g(\xi^i_{n,2}(m,x),t) \\
&- \sum_{p=1}^{n-1} \frac{G_{p+1} - G_p}{2} (g(\xi^i_{n,2p+1}(m,x),t) + g(\xi^i_{n,2p+2}(m,x),t))\} \\
&- \sum_{m=0}^{+\infty} \{G_n g(\eta^i_{n,1}(m,x),t) - G_1 g(\eta^i_{n,2}(m,x),t) \\
&- \sum_{p=1}^{n-1} \frac{G_{p+1} - G_p}{2} (g(\eta^i_{n,2p+1}(m,x),t) + g(\eta^i_{n,2p+2}(m,x),t))\}.
\end{aligned} \tag{8}$$

B. The compact EM model and time to failure calculation

We notice that the solution in (8) contains an infinite number of terms. One observation we have with Laplace transformation based solution with the infinite number of terms is that we may just need a few dominant terms for sufficient accuracy. Fortunately, we show in experimental section that this is indeed a case for our problem. For instance, we just keep the first dominant term $(m = 0)$, then the solution for the i-th $(i = 1, 2, \cdots, n)$ segment, can be re-written as:

$$\begin{aligned}
\sigma_i(x,t) \approx &-\{G_n g(\xi^i_{n,1}(0,x),t) - G_1 g(\xi^i_{n,2}(0,x),t) \\
&- \sum_{p=1}^{n-1} \frac{G_{p+1} - G_p}{2} (g(\xi^i_{n,2p+1}(0,x),t) + g(\xi^i_{n,2j+2}(0,x),t))\} \\
&- \{G_n g(\eta^i_{n,1}(0,x),t) - G_1 g(\eta^i_{n,2}(0,x),t) \\
&- \sum_{p=1}^{n-1} \frac{G_{p+1} - G_p}{2} (g(\eta^i_{n,2p+1}(0,x),t) + g(\eta^i_{n,2p+2}(0,x),t))\}.
\end{aligned} \tag{9}$$

By just use a few dominant terms, we can obtain the very compact EM stress development models for the multi-segment interconnect wires. It should be noted that when the wire segment stress $\sigma_i(x,t)$ reaches a critical stress σ_{crit}, then the void nucleation time t_{nuc} can be calculated for each segment by solving the equation $\sigma_i(x, t_{nuc}) = \sigma_{crit}$.

IV. Experimental results and discussions

In order to show the accuracy of the proposed model of EM reliability for multi-branch interconnect tree with line structure shown in Fig. 3, the analytical solution (8) of stress evolution equations is implemented in the MATLAB environment, and we also compare the results from (8) with those obtained by the finite element tool COMSOL [21]. In our experiments, due to the limitation of space, we test two cases of interconnect tree structure by changing n in (8) which is the number of wire segments in the interconnect tree. In the simulations to be described below, the following parameter values will be used: $Z^* = 10$, $\rho = 3 \times 10^{-8} \Omega/m$, $\Omega = 8.78 \times 10^{-30} m^3$, $B = 5.2 \times 10^{10} Pa$, $D_0 = 5.5 \times 10^{-5} m^2/s$, $E_a = 1.1eV$, $e = 1.6 \times 10^{-19} C$, $k = 1.38 \times 10^{-23} J/K$, and $T = 350K$.

A. Four-terminal interconnect wire ($n = 3$)

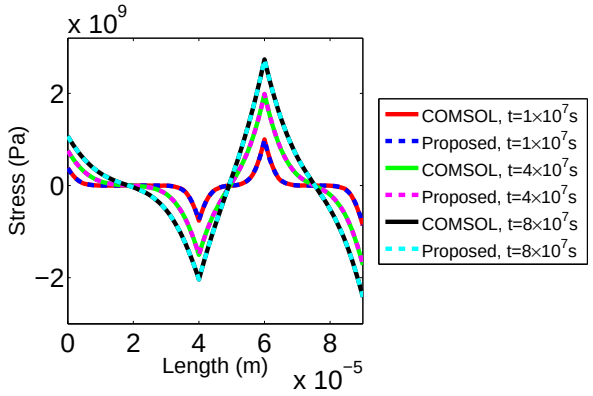

Fig. 4. EM-induced stress evolution along the four-terminal interconnect wire ($n = 3$).

We first analyze the four-terminal interconnect tree with three wire segments $(n = 3)$ as shown in Fig. 3. For this type of interconnect wire, the integer n in the stress evolution equation (3) is set to be 3. For our simulation, a constant current density of $j_1 = 2.2 \times 10^{10} A/m^2$ is applied in the left segment, while a current density with varying direction and magnitude, $j_2 = -6.6 \times 10^{10} A/m^2$ is used to stress the middle wire segment. The current density of the right wire segment is set to be $j_3 = 5 \times 10^{10} A/m^2$. The positions for this four-terminal interconnect wire are set to be $l_0 = 0 \times 10^{-5} m$, $l_1 = 4 \times 10^{-5} m$, $l_2 = 6 \times 10^{-5} m$, and $l_3 = 9 \times 10^{-5} m$, respectively. Fig. 4 shows the EM stress development calculated by employing the one-term approximation form of the exact series solution (8) for the three-segment interconnect wire, in comparison with the finite element analysis results obtained from COMSOL. It can be seen from Fig. 4 that the analytical solution obtained with the proposed method fits well to the results of the numerical simulation at every time instance.

Localized tensile and compressive stresses are generated from the EM-induced material depletion and accumulation at the locations of atom flux divergence. The resulting stress gradient leads to a backflow flux of atoms to oppose the EM flux. For the void nucleation phase, EM-induced voids will not form if the balance between the backflow and EM fluxes can be achieved before the tensile stress value along the metal wire reaches the critical stress boundary. In this situation, the wire interconnect structure is virtually immortal. The wire will be immortal if the maximum steady-state stress is less than the critical stress σ_{crit}. It is observed from Fig. 5 that the steady-state stress distributions from the proposed analytical model match well with the COMSOL simulation results.

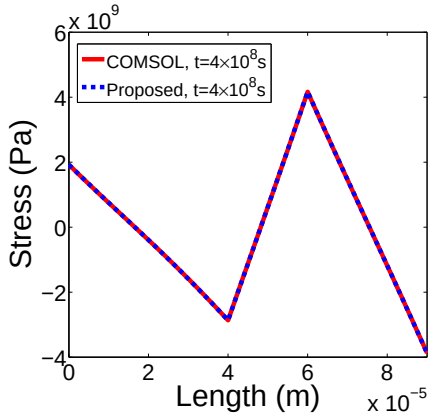

Fig. 5. Steady-state stress distributions along the four-terminal interconnect wire ($n = 3$).

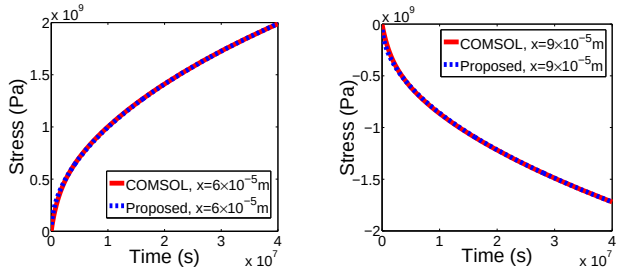

(a) (b)

Fig. 6. EM-induced stress development over time for the four terminal interconnect wire: (a) the tensile stress at the position $x = 6 \times 10^{-5}m$; (b) the compressive stress at the position $x = 9 \times 10^{-5}m$.

It should be noted that the current direction in the middle segment is opposite to the direction of the currents in the left and right segments. As a result, both the tensile and compressive stresses can be generated along this three-segment interconnect wire. Fig. 6(a) and Fig. 6(b) show the developments of the tensile stress at the position $x = 6 \times 10^{-5}m$ and the compressive stress at the position $x = 9 \times 10^{-5}m$, respectively. It can be seen from Fig. 6 that both the tensile and compressive stresses calculated by the proposed analytical model matches well the COMSOL simulation results.

B. Six-terminal interconnect wire ($n = 5$)

Now we calculate the EM-induced stress evolution by the proposed analytical model for the six-terminal interconnect wire. For this type of interconnect wire, the integer n in the closed-form expression (8) equals to 5. For the simulation of stress evolution during the void nucleation phase, the current densities in each segment are set to be $j_1 = 2 \times 10^{10}A/m^2$, $j_2 = -4 \times 10^{10}A/m^2$, $j_3 = 6 \times 10^{10}A/m^2$, $j_4 = -5 \times 10^{10}A/m^2$, and $j_5 = 1 \times 10^{10}A/m^2$, respectively. The positions $l_i (i = 0, 1, \cdots, 5)$ in (8) for this five-segment wire are chosen as $l_0 = 0 \times 10^{-5}m$, $l_1 = 2 \times 10^{-5}m$, $l_2 = 3 \times 10^{-5}m$, $l_3 = 6 \times 10^{-5}m$, $l_4 = 8 \times 10^{-5}m$, and $l_5 = 10 \times 10^{-5}m$, respectively. We use the one-term approximation of the exact series solution (8) to calculate the EM-induced stress development along this five-segment wire. Fig. 7 shows the time evolution of the stress during the void nucleation phase. It can be seen from Fig. 7 that the obtained results are in good agreement with the finite element simulation results.

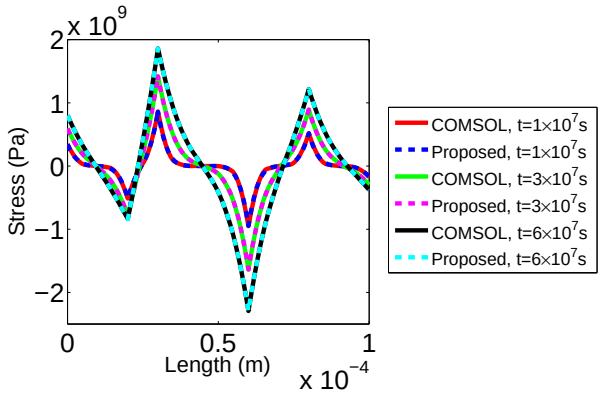

Fig. 7. EM-induced stress development along the six-terminal interconnect wire ($n = 5$).

As mentioned above, if the critical stress σ_{crit} during the void nucleation phase is greater than the maximum steady-state tensile stress value along the five-segment interconnect wire, it is immortal, i.e., no voids will form in the wire and it will never fail. Fig. 8 shows the steady-state stress distributions along the wire, from which we can see that the analytical solution can fit well with the COMSOL simulation results. It should be noted that the first, third, and fifth segments in the line wire have the same current direction that is opposite to the direction of the currents in the second and fourth segments. As a result, both the tensile and compressive stresses can be generated in this interconnect wire. Fig. 9(a) and Fig. 9(b) show the compressive stress development over time at the position $x = 6 \times 10^{-5}m$ and the tensile stress development at $x = 8 \times 10^{-5}m$, respectively. Again, the obtained results from the one-term approximation of the exact series solution match well with the numerical simulation results calculated by COMSOL.

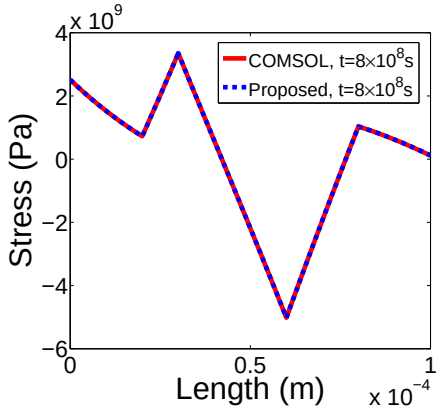

Fig. 8. Steady-state stress distributions along the six-terminal interconnect wire ($n = 5$).

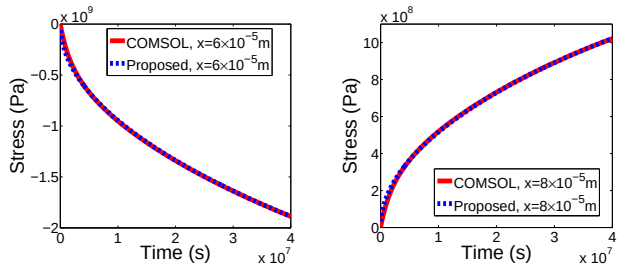

(a) (b)

Fig. 9. EM-induced stress development over time for the six-terminal interconnect wire: (a) the compressive stress at the position $x = 6 \times 10^{-5} m$; (b) the tensile stress at the position $x = 8 \times 10^{-5} m$.

C. Accuracy study for the analytic model

We now study the accuracy of the proposed analytic model using the one-term approximation of the exact series solution against the COMSOL simulation results. Due to limited space, only the results for the three-segment wire case are shown in the paper. The relative errors are plotted in Fig. 10 against the COMSOL simulation results for the case using the one-term approximation, i.e., the integer m in the series solution (8) is set to be zero. As we can see from Fig. 10, the resulting relative errors between the one-term approximation and the COMSOL simulation results are around 2%. In the experiments we noted that the accuracy cannot be improved significantly by adding more terms, which means that the one-term approximation is enough to calculate the EM-induced stress during the void nucleation phase for this three-segment interconnect tree.

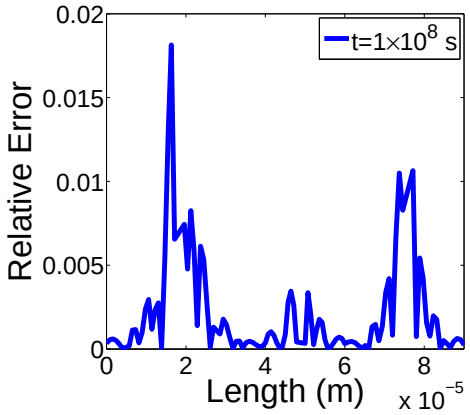

Fig. 10. Relative errors between the proposed analytical model and the COMSOL model for the three-segment interconnect wire.

V. Conclusion

In this paper, we have proposed a new analysis method for multi-segment wires considering EM effects during the void nucleation phase, which can be used for practical VLSI interconnect design techniques. An exact series solution to the stress evolution equation for multi-segment wires has been derived by using the Laplace transformation technique. The obtained physics-based analytic EM model results are in good agreement with the calculation by the finite element analysis tool COMSOL. Experiment results demonstrate that using the first dominant term approximation of the exact series solution can lead to around 2% error, which satisfies the requirement of practical EM reliability analysis.

References

[1] "International technology roadmap for semiconductors (ITRS), 2014 update," 2012. http://public.itrs.net.

[2] B. Bailey, "Thermally Challenged," in *Semiconductor Engineering*, 2013.

[3] R. De Orio, H. Ceric, and S. Selberherr, "Physically based models of electromigration: From blacks equation to modern tcad models," *Microelectronics Reliability*, vol. 50, no. 6, pp. 775–789, 2010.

[4] I. A. Blech, "Electromigration in Thin Aluminum Films on Titanium Nitride," *Journal of Applied Physics*, vol. 47, no. 4, pp. 1203–1208, 1976.

[5] J. R. Black, "Electromigration-A Brief Survey and Some Recent Results," *IEEE Trans. on Electron Devices*, vol. 16, no. 4, pp. 338–347, 1969.

[6] M. Ohring, *Reliability and Failure of Electronic Materials and Devices*. San Diego: Academic Press, 1998.

[7] J. R. Lloyd, "New models for interconnect failure in advanced IC technology," *Physical and Failure Analysis of Integrated Circuits, 2008. IPFA 2008. 15th International Symposium on the*, pp. 1–7, 2008.

[8] M. Hauschildt, C. Hennesthal, G. Talut, O. Aubel, M. Gall, K. B. Yeap, and E. Zschech, "Electromigration Early Failure Void Nucleation and Growth Phenomena in Cu And Cu(Mn) Interconnects," in *IEEE International Reliability Physics Symposium (IRPS)*, pp. 2C.1.1–2C.1.6, 2013.

[9] J. S. Pak, M. Pathak, S. K. Lim, and D. Pan, "Modeling of electromigration in through-silicon-via based 3D IC," in *Electronic Components and Technology Conference (ECTC), 2011 IEEE 61st*, pp. 1420–1427, 2011.

[10] M. Pathak, J. S. Pak, D. Pan, and S. K. Lim, "Electromigration modeling and full-chip reliability analysis for BEOL interconnect in TSV-based 3D ICs," in *Computer-Aided Design (ICCAD), 2011 IEEE/ACM International Conference on*, pp. 555–562, 2011.

[11] X. Zhao, Y. Wan, M. Scheuermann, and S. K. Lim, "Transient modeling of TSV-wire electromigration and lifetime analysis of power distribution network for 3D ICs," in *Computer-Aided Design (ICCAD), 2013 IEEE/ACM International Conference on*, pp. 363–370, 2013.

[12] J. Pak, S. K. Lim, and D. Z. Pan, "Electromigration study for multi-scale power/ground vias in TSV-based 3D ICs," in *Computer-Aided Design (ICCAD), 2013 IEEE/ACM International Conference on*, pp. 379–386, 2013.

[13] X. Huang, T. Yu, V. Sukharev, and S. X.-D. Tan, "Physics-based electromigration assessment for power grid networks," in *Proc. Design Automation Conf. (DAC)*, June 2014.

[14] M. A. Korhonen, P. Borgesen, K. N. Tu, and C. Y. Li, "Stress Evolution Due to Electromigration in Confined Metal Lines," *Journal of Applied Physics*, vol. 73, no. 8, pp. 3790–3799, 1993.

[15] H. Chen, S. X.-D. Tan, V. Sukharev, X. Huang, and T. Kim, "Interconnect reliability modeling and analysis for multi-branch interconnect trees," in *Proc. Design Automation Conf. (DAC)*, June 2015.

[16] H. Chen, X. Tan, X. Huang, T. Kim, and V. Sukharev, "Analytical modeling and characterization of electromigration effects for multi-branch interconnect trees," *IEEE Trans. on Computer-Aided Design of Integrated Circuits and Systems*, vol. 35, pp. 1811–1824, Nov. 2016.

[17] J. J. Clement, S. P. Riege, R. Cvijetic, and C. V. Thompson, "Methodology for Electromigration Critical Threshold Design Rule Evaluation," *IEEE Trans. on Computer-Aided Design of Integrated Circuits and Systems*, vol. 18, no. 5, pp. 576–581, 1999.

[18] V. Sukharev, X. Huang, and S. X.-D. Tan, "Electromigration Induced Stress Evolution Under Alternate Current and Pulse Current Loads," *Journal of Applied Physics*, vol. 118, pp. 034504–1–034504–10, 2015.

[19] X. Huang, A. Kteyan, X. Tan, and V. Sukharev, "Physics-based electromigration models and full-chip assessment for power grid networks," *IEEE Trans. on Computer-Aided Design of Integrated Circuits and Systems*, vol. 35, pp. 1848–1861, Nov. 2016.

[20] Z. Sun, E. Demircan, T. Kim, X. Huang, T. Kim, and S. X.-D. Tan, "Voltage-based electromigration immortality check for general multi-branch interconnects," in *Proc. Int. Conf. on Computer Aided Design (ICCAD)*, 2016.

[21] "Comsol multiphysics." http://www.comsol.com.